Key Engineering Materials Vols. 261-263 (2004) pp. 177-182
online at http://www.scientific.net

The Role of Constraint and Warm Pre-stress on Brittle Fracture in Ferritic Steels

A.Mirzaee-Sisan, S.Hadidi-moud, C.E. Truman and D.J. Smith

Department of Mechanical Engineering, University of Bristol
Queen's Building, Bristol, BS8 1TR,UK

Keywords: Brittle fracture, failure probability, local approach, triaxiality

ABSTRACT

This paper presents the results of an experimental and numerical study carried out to investigate the effect of warm pre-stressing on cleavage fracture in ferritic steels using cracked and notched specimens. It is shown that the local approach based on Weibull theory predicts the increase in toughness following warm pre-stressing in highly constrained geometries. The observed effect of pre-loading in low constraint specimens such as round notched bars is less. The local approach could not predict the differences and it is suggested that the variation of triaxiality factor, the ratio of hydrostatic stress to Von Mises, in the plastic zone, is a contributing factor.

1. INTRODUCTION

Warm pre-stressing (WPS) is commonly demonstrated by the Loading-Unloading-Cooling-Fracture (LUCF) load-temperature cycle. It is known that loading and unloading a cracked component at room temperature can enhance its subsequent load bearing capacity at low temperature. Recently Hadidi-Moud et al [1] applied the "local" approach to predict the effect of warm pre-stress on brittle fracture. In their approach Weibull parameters are required. These were calibrated with the aid of finite element analysis using experimental results for as-received (AR) material at low temperature. The same parameters were then used to predict the warm pre-stress effect. The present work follows the same procedure and focuses on attaining an understanding of the role of constraint in the calibration of Weibull parameters and level of improvement in load bearing capacity following warm pre-stressing.

The basis for the "local" approach is the Beremin model [2]. It is assumed that micro-cracks occur at the onset of plastic deformation and that unstable fracture takes place when the maximum principal stress reaches a critical level. In other words, the plastic deformation is referred to as a primary event prior to failure. Global failure is predicted by invoking the weakest link theory. This assumes that a body of material can be fragmented into many independent volumes, linked together like a chain, and the failure of a body commences when its weakest element link fails.

The modified Beremin four-parameter model with inclusion of a minimum threshold stress, σ_{min} is given by:

$$P_f\left[\sigma_f\right] = 1 - exp\left[-\left(\frac{\sigma_w - \sigma_{min}}{\sigma_u - \sigma_{min}}\right)^m\right] \qquad (1)$$

where σ_w, the Weibull stress, is:

$$\sigma_w = \left[\sum_{i=1}^{n_{pl}} \left(\sigma_1^i\right)^m \frac{\Delta V_i}{V_0} \right]^{1/m} \quad (2)$$

The Weibull stress, σ_w, is a characteristic stress obtained by integration of the maximum principal stresses over the plastic zone, consisting of n_{pl} elements and scaled by a reference volume, V_0. The reference stress, σ_u, corresponds to a failure probability of 63.2% and is referred to as the mean stress. The exponent "m" describes the scatter in the fracture test data. Finally, the threshold stress, σ_{min}, is included in the original Beremin model to achieve a better fit to the fracture data.

In the original Beremin approach, the exponent "m" and the reference stress σ_u were first calibrated using a database of experimental data collected from a wide range of round notched bar (RNB) specimens with various notch tip geometry and tested at different temperatures. It was suggested that the same parameters were appropriate in predicting scatter in fracture data for other configurations including specimens with different geometry and containing sharp cracks. Beremin also suggested that the reference volume, V_0, was a volume equivalent to about ten grains, typically $V_0=0.001$ mm^3. However, Hadidi-Moud et al [1] suggested that V_0 is an arbitrary scaling parameter.

The intention in this study is to investigate the dependency of these parameters for specimens with different level of triaxiality (or constraint). In the following section results from a series of experiments are presented. This is followed by finite element studies and detailed probability analysis. In section 5 results are examined in terms of triaxiality factor to illustrate the different levels of specimen constraint. The transferability of the Weibull parameters between different specimens with different level of triaxiality is discussed.

2. EXPERIMENTS

Earlier experimental results for twenty eight A533B specimens were obtained by Smith and Garwood [3] using single edge notch bend SEN(B) specimens containing fatigue pre-cracks with nominal a/W=0.5 and $W=2B=100$ mm. Fourteen specimens in the as-received condition were loaded to fracture at -170°C with another fourteen in the warm pre-stressed condition at same temperature. The WPS cycle was applied by loading at room temperature equivalent to an elastic stress intensity factor of 120MPa√m and then unloading to zero load and cooled to –170°C before being reloaded to fracture.

Recent results of A508 steel using round notched bar (RNB) specimens tested in the AR and WPS conditions at -150°C are summerised here. Thirty four RNB specimens were extracted from a block of A508 Class3 C-Mn steel in the S-L orientation. Sharp (V) and shallow (U) circumferential notches were introduced into the mid section of the specimens. The tip radius of 'U' shape notches was 1.25mm, and 0.07mm for 'V' notches. The sharp notch was introduced by using electro-discharge machining. For the remaining of the paper RNB-U1.25 refers to the shallow notch and RNB-V0.07 to the sharp notch. For each notch tip geometry, fracture tests were carried out at –150^{o}C in the as-received and warm pre-stressed conditions. The pre-load level at room temperature was equivalent to a net section stress of 994 MPa.

The results of SEN(B) in terms of fracture toughness and net section stresses for RNB specimen are shown against the failure probability in Fig.2 and Fig.3 respectively. The failure probability P_f for experimental results was determined using:

$$P_f = \frac{i - 0.5}{N} \tag{3}$$

where N is the total number of specimens, and i the rank or order number.

Using a scanning electron microscope it was observed that all specimens failed by cleavage fracture. The experimental results from the pre-cracked SEN(B) specimens demonstrated that there was a considerable improvement in fracture toughness following WPS. The results from the RNB tests did not show the same level of improvement. The increase in the average fracture stress in RNB-U1.25 was negligible. Nevertheless, the minimum fracture stress for RNB-U1.25 raised from 1231MPa to 1359 MPa. It is noticeable that the RNB-V0.07 specimens show more improvement in fracture stress compared with RNB-U1.25.

3. FINITE ELEMENT SIMULATION

Finite element analyses were performed to provide input data to an analysis that used the local approach to predict failure conditions. The commercial code ABAQUS CAE (V 6.2) was used to create the finite element models. To take advantage of symmetry, one quarter of RNB specimens, shown in Fig.1 were modeled using axi-symmetric quadratic eight node elements with reduced integration (CAX8R).

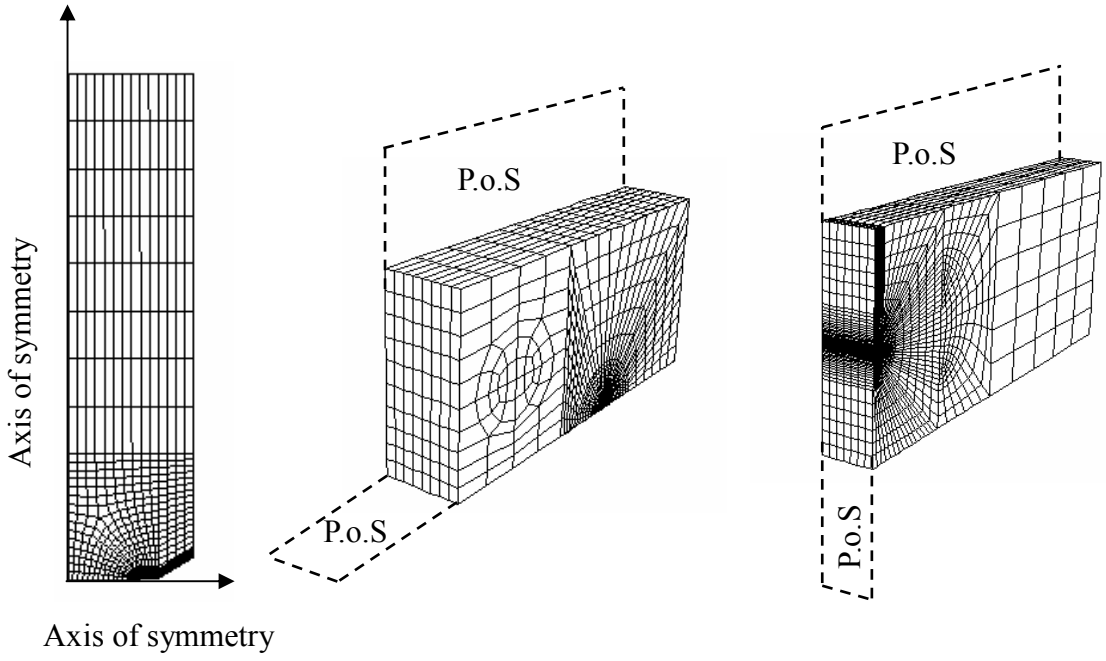

Fig.1. Details of FE mesh: RNB(Left); C(T)(middle); SEN(B)(Right)

P.o.S: Plane of Symmetry

For the pre-cracked specimens 3-D models of SEN(B) *W=2B=100* mm and a C(T) *W=2B=50* mm were created. All models contained a refined mesh around the crack tip. Two symmetry planes allowed one quarter of the specimens to be modeled, and eight node elements with reduced integration (C3D8R) were used. The FE models are shown in Fig.1.

An elastic-plastic material model with isotropic hardening was used for all analyses. For A533B

steel the yield strengths (0.2% offset) were 528MPa and 877MPa at 20°C and -170°C respectively. For A508 steel the yield strengths were 430MPa at 20°C and 695MPa at -150°C.

4. PROBABILITY ANALYSIS

4.1. Calibration of the Weibull parameters

It was first necessary to calibrate the Weibull parameters, m, V_0, σ_u and σ_{min}. To estimate probability of fracture a routine developed by Hadidi-Moud et al [1] was used in conjunction with the results from the FE analyses. A region around the crack/notch tip was chosen as a "fracture process zone" and modeled with a fine mesh in the finite element analysis. This zone was large enough to include all the elements that undergo plastic deformation during loading to fracture.
The experimental data of pre-cracked specimens carried out by Garwood-Smith [3] were available for SEN(B), B=50 mm. These data can be converted for use with the C(T), B=25 mm model based on the toughness dependence with specimen thickness as follows [4]:

$$\frac{K_{B1}}{K_{B0}} = \left(\frac{B_0}{B_1}\right)^{1/4} \tag{4}$$

where K_{B1} and K_{B0} are the fracture toughness corresponding to B_1 and B_0 (the reference thickness).

FE models for both specimens have been analysed. The incremental stress distributions during loading to fracture were used as input for the routine and the Weibull parameters were calibrated using the AR data. Like Hadidi-Moud et al [1] the shape factor m and reference volume were chosen as *4* and *0.01 mm*^{3} respectively. Using either model a good fit was attained by choosing σ_u*=10.30GPa* and σ_{min}*=3.5GPa*.

The fracture behaviour of RNB specimen was also studied using two different notch tip sharpness. In calibration of Weibull parameters (m, σ_u and σ_{min}) for RNB-U1.25 a reference volume was fixed to magnitude of *0.001 mm*^{3}. The parameters that provide the best agreement with experimental results at –150°C were *m=24*, σ_u *=3.16GPa* and σ_{min} *=0.8GPa*. Using these values, the probability of fracture at –150 ^{0}C shown in Fig.3 was obtained. The same procedure was repeated for RNB-V0.07 and the best agreement with the experimental results was achieved for *m=8,* σ_u *=4.98GPa* and σ_{min} *=0.0GPa* as shown in Fig.3.

The sets of Weibull parameters were then used to predict the enhancement in cleavage fracture stress following the LUCF cycle for both temperatures.

4.2. Prediction of the Warm pre-stress effect

The WPS was simulated by loading and unloading the FE model using the elastic-plastic material properties at room temperature. This was followed by reloading to fracture using the lower temperature elastic-plastic mechanical properties. For the pre-cracked specimens only C(T), B=25 mm model and the "local" routine [1] were used together with the calibrated Weibull parameters to the as-received fracture behaviour, to predict the WPS effect on fracture toughness. Both RNB-U1.25 and RNB-V0.07 models were analysed for the prediction of WPS effect on fracture stress. For pre-cracked specimens the local approach predicted significant improvement in toughness following proof loading and a good agreement was found between the prediction of the local approach and the experiments. The results from the WPS simulations for A508 steel RNB specimens are shown in Fig.3. For RNB-U1.25 the simulation predicted an improvement in the fracture stress at low stresses whereas the average of fracture stress remained unchanged.

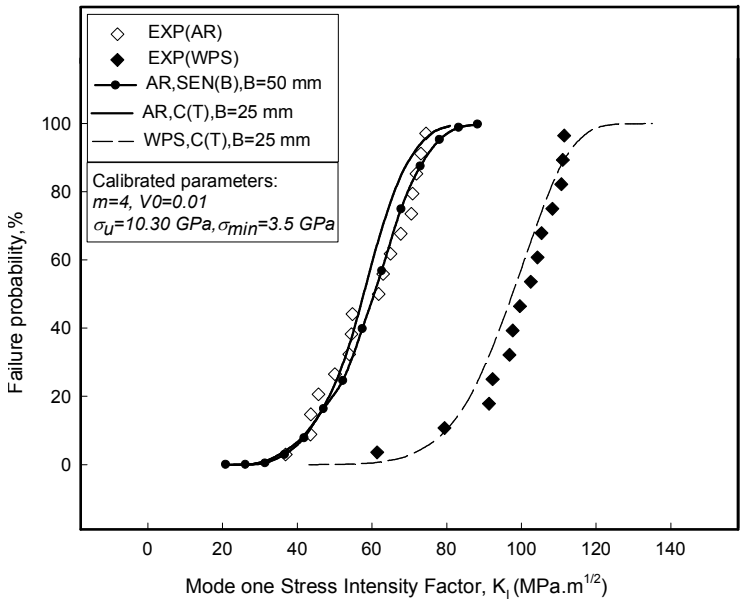

Fig.2. Prediction of failure probability for as-received and warm pre-stressed conditions for A533B

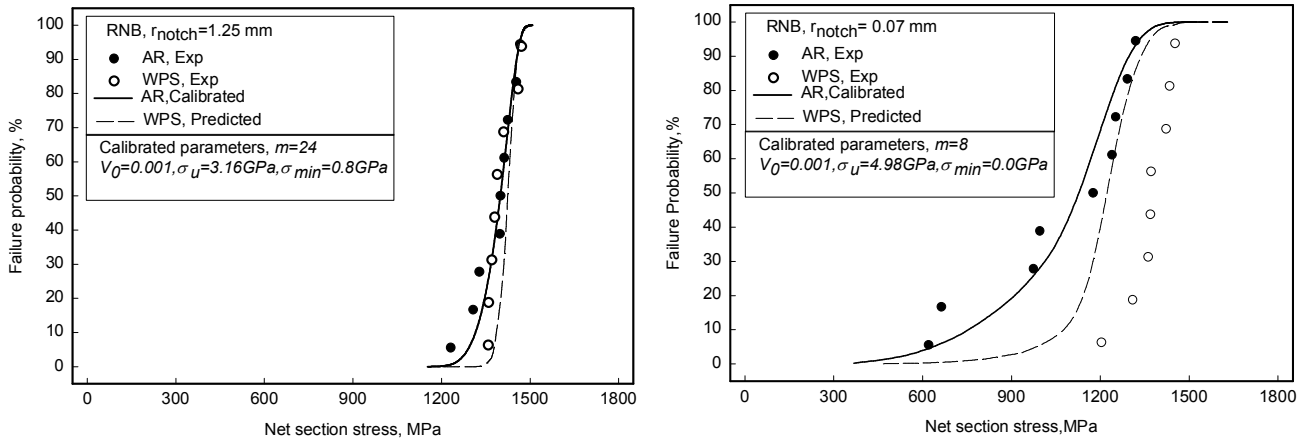

Fig.3. Prediction of failure probability for as-received and warm pre-stressed conditions for A508:

RNB-U1.25 (left); RNB-V0.07 (right)

The model also predicted improvements in fracture stress following WPS for RNB-V0.07. However the predicted enhancement was not as much as the experiments suggested.

5. THE ROLE OF CONSTRAINT

Millela and Bonora [5] argued that a change in triaxiality would have an impact on the value of m since localised triaxiality determines the extent of the process zone. The triaxiality factor T_f is given by the ratio of hydrostatic stress to Von Mises equivalent stress: The relationship between m and T_f was obtained from experiments is given by:

$$m = 55.4 - 22.4\left(T_f\right) \qquad (5)$$

Here the triaxiality factor has been used as an indicator of the level of constraint between different

specimens. Fig. 4 shows the incremental variation of triaxiality factor in the plastic zone during loading to fracture in as-received condition. The Weibull stresses were calculated based on integration of principal stress within the plastic zone. Similarly the variation in triaxiality factor was also calculated in the plastic zone. The triaxiality factors in pre-cracked specimens including C(T), B=25 and SEN(B), B=50 are very close to each other. Therefore the same value of m was used for all. The magnitude of the calibrated m and the level of triaxiality appeared to satisfy equation 5.The triaxiality factor in RNB-U1.25 is lower than RNB-V0.07 and for both RNB specimens less than pre-cracked specimens. Furthermore finite element analysis also showed that the whole net section of round notched bar undergoes plastic deformation prior to fracture. This implies that the effect of WPS is wiped out in the presence of large plastic deformation, which was the case for RNB specimens with low constraint. It is noted that the calibrated and predicted m values using Milella and Bonora [5] are in fairly good agreement in RNB and pre-cracked specimens.

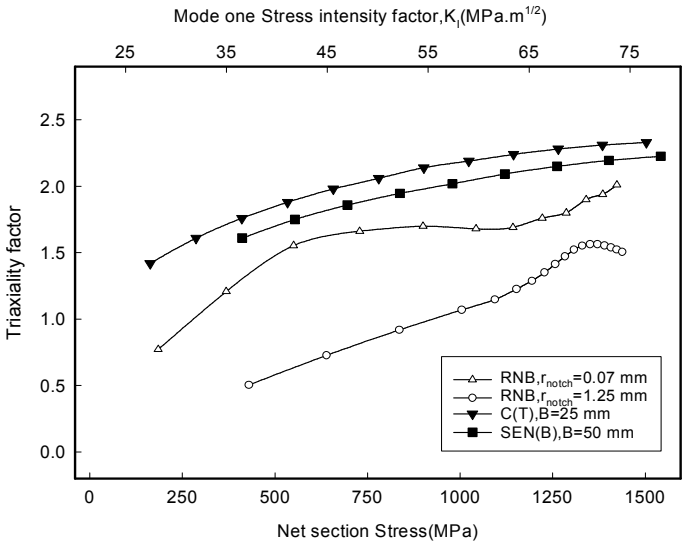

Fig. 4. Maximum of triaxiality factors in the plastic zone

during loading to fracture in as-received condition

6. CONCLUSIONS

Hojo et al [6] suggested that the Weibull parameters are independent of geometry. Here we show that the calibrated Weibull parameters for RNB cannot be directly applied to highly constrained specimens. Following LUCF load cycle there is improvement in apparent toughness in highly constrained specimens. Lower triaxiality factors can also explain why the warm pre-stressing does not have a major effect for the RNB specimen.

REFERENCE

1. S. Hadidi-Moud, A. Mirzaee-Sisan, C.E. Truman and D.J. Smith, PVP Conf., Canada, Vancouver, **434** (2002) p.111
2. F.M. Beremin, J. Metall. Trans. **14A** (1983) p. 2277
3. D.J. Smith, S.J. Garwood, Int. J. Pres. Ves. & Piping, **41** (1990) p.297
4. K.Wallin, Engng. Fract. Mech, **22**(1985) p.149
5. P.P. Milella, N. Bonora, Int. J. Fracture, **104** (2000) p.71
6. K. Hojo, I. Muroya, A. Bruckner-Foit, Nuclear Eng & Design, **174** (1997) p.247